

# Enhancement of Airfoil Aerodynamic Characteristics by Surface Modifications

Elhassen Ali Ahmed Omer<sup>1\*</sup> , Hana Mofteh Momen<sup>2</sup>, Rayan Nassr Yahia<sup>2</sup>

<sup>1</sup>Zawia University, Faculty of Engineering, Mechanical Engineering Department.

<sup>2</sup>Tripoli University, Faculty of Engineering, Aeronautical Engineering Department.

\*Corresponding author email: e.amr@zu.edu.ly

Received: 18.11.2023 | Accepted: 09.12.2023 | Available online: 15-12-2023 | DOI:10.26629/uzjest.2023.06

## ABSTRACT

The enhancement of the aerodynamic characteristics of the NACA0012 airfoil is studied numerically. ANSYS Fluent is used to simulate the airfoil's performance by applying certain surface modifications in the form of dimples and protrusions. Different shapes were used, namely, semicircular, v-shaped and square. Analysis has been done on an airfoil of 1m chord length with these modifications, which were implemented on the upper surface of a two-dimensional airfoil model and placed at 75% of chord length. A comparative study of surface-modified airfoil models was done to investigate lift and drag for a constant at  $Re = 3.0E6$  at various angles of attack and compare them with smooth airfoils. The results reveal that the aerodynamic characteristics were improved by applying surface modifications, and the flow separation on the airfoil can be delayed by using dimples and protrusions on the upper surface. It was found that the semicircular dimples and v-shaped bumps have the best aerodynamic enhancement, where the lift coefficient was improved by 11% and 9% compared to smooth airfoils, respectively, while the drag coefficients were reduced by 3% for both shapes. Also, based on these surface-modified airfoil analyses, the stall angle was increased by two degrees. In comparison, the semicircular dimples are more suitable for enhancing the performance characteristics of airfoils.

**Keywords:** Airfoil, lift, drag, surface modification, dimples

## تعزيز الخصائص الديناميكية الهوائية عن طريق تعديلات سطح الجنيح

الحسن علي أحمد عمرو<sup>1</sup> ، ، هناء مفتاح مؤمن<sup>2</sup> ، ريان نصر يحي<sup>2</sup>  
قسم الهندسة الميكانيكية والصناعية، كلية الهندسة جامعة الزاوية، الزاوية، ليبيا.  
قسم هندسة الطيران ، كلية الهندسة جامعة طرابلس، طرابلس، ليبيا.

## ملخص البحث

في هذا البحث تم دراسة تحسين الديناميكا الهوائية للتدفق فوق الجنيح NACA 0012 من خلال تطبيق برنامج CFD Code ANSYS Fluent. تم إجراء تعديلات معينة على السطح في شكل غمازات ونبوءات باستخدام أشكال مختلفة وهي: نصف دائري، على شكل حرف V، ومربع، وتم تنفيذ هذه التعديلات على السطح العلوي لنموذج الجنيح ثنائي الأبعاد، وعلى بعد 75% من طول الوتر ومقارنته بالجنيح الأملس. وأظهرت النتائج أن خصائص الديناميكية الهوائية قد تم تحسينها من

خلال إجراء هذه التعديلات السطحية وذلك أن فصل الجريان على الجنيح يمكن تأخيره باستخدام الغمازات والنتوءات على السطح العلوي، وقد وجد أن الغمازات نصف الدائرية والنتوءات على شكل حرف V الأفضل لتحسين الخصائص الديناميكية الهوائية وذلك بزيادة معامل الرفع بنسب 11% و 9% عن الجنيح الأملس على التوالي. بينما انخفضت معاملات السحب بنسبة 3%، وزادت AOA بمقدار درجتين لكلا الشكلين. وبالمقارنة تعتبر الغمازات نصف الدائرية أكثر ملاءمة لتحسين خصائص الديناميكية الهوائية، مما يوفر أداءً معززاً للجنيحات.

**الكلمات الدالة:** الجنيح، الرفع، قوة الجر، قوة الإعاقة، تعديل السطح، غمزاوات.

## 1. Introduction

An airfoil is the cross-section of an aircraft wing. The flow of a round airfoil surface at low velocities or low angles of attack is laminar, so it remains attached to the surface, and symmetric airfoils cannot generate much lift force. At higher angles of attack, the flow becomes turbulent, leading to a higher pressure difference between the surface sides of the airfoil. Therefore, a higher lift is generated until the critical angle of attack is reached, known as the stall angle, where the maximum lift force is produced. After stall angle, the lift drops down while the drag increases faster due to the adverse pressure gradient generated as a result of flow separation from the airfoil surface. Therefore, controlling the flow separation is considered an effective method to improve the aerodynamic characteristics of the foil.

Flow control in aerodynamics is used to manipulate flows over airfoils by passive or active techniques to improve the aerodynamic airfoils performances, that is, lift augmentation, drag reduction, noise minimization and avoiding or postponing boundary layer separation. The active methods involve external power, whereas the passive methods use surface or geometrical modifications [1, 2]. Surface modifications are vital in improving the aerodynamic performance of an airfoil, and they are really effective in altering the boundary layer by creating vortices, which delay the boundary layer separation, resulting in a decrease in pressure drag and an increase in the angle of stall. Many researchers investigated the effect of dimples on the upper, lower and both airfoil surfaces, both numerically and experimentally. Different types of airfoils were used in their investigation. They found that dimples reduce the drag and produce turbulence that delays the separation of the boundary layer, decreases the formation of the wake and increases the stall angle. The pressure distribution around the airfoil surface indicates the presence of separation, which is delayed by dimples [3-7]. Experimental and numerical investigations for different types of airfoils were carried out [8, 9], a good agreement was obtained between the experimental and numerical results. Their parametric study shows that a higher maximum lift coefficient is achieved when the VG is placed near the separation point. Also, an experimental study of NACA 4415 and NACA 4412 airfoils equipped with vortex generators placed on the suction side of the airfoils to control the flow separation.

The results show that triangular-shaped vortex generators are best suited to control boundary layer separation [10, 11]. The aerodynamic efficiency of the NACA 0012 airfoil was investigated [12-14], the airfoil surface with and without dimples was studied experimentally. Dimples and protrusions used as a passive technique are placed at 30% c from the trailing edge at the upper surface. The experiments were carried out under different Reynolds numbers for various angles of attack from 0 to 23. It was found that the efficiency of the airfoil improves with the dimples. Also, the results proved that using that technique leads to a reduction in the drag and an increase in the lift; therefore, there is a large improvement in the aerodynamic performance of the airfoil. The locations of inward and outward dimples were investigated [15, 16]. Different locations chordwise were tested, and their results revealed a 75% c location increase in lift coefficient by 17% and a reduction in drag coefficient by 6%.

In this study, a passive technique was used to control the separation of the boundary layer using surface modifications. Dimples and protrusions of different shapes were attached to the upper surface of the NACA0012 profile to improve its aerodynamic performance. ANSYS Fluent was used to solve the Newtonian, compressible and two-dimensional RANS equations with the SST k- $\omega$  turbulence model. The optimal position and dimension of the vortex generators were determined based on the results of [15]. The study was carried out for  $Re = 3.0E+6$  and a range of angles of attack  $0 - 20^\circ$ .

## 2. Mathematical Modelling

The incompressible, two-dimensional steady Reynolds averaged Navier-Stokes (RANS) equations were employed. RANS equations can be written as [17]:

$$\frac{\partial}{\partial x_i} (\rho u_i) = 0 \quad (1)$$

$$\frac{\partial}{\partial x_j} (\rho u_j u_i) = -\frac{\partial p}{\partial x_i} + \frac{\partial}{\partial x_j} \left[ \mu \left( \frac{\partial u_i}{\partial x_j} + \frac{\partial u_j}{\partial x_i} \right) \right] + \frac{\partial}{\partial x_j} (-\rho \overline{u'_i u'_j}) \quad (2)$$

The normal Reynolds stress, which is combined by the Boussinesq relationship and the eddy viscosity is given by:

$$-\rho \overline{u'_i u'_j} = \mu_t \left( \frac{\partial u_i}{\partial x_j} + \frac{\partial u_j}{\partial x_i} \right) \quad (3)$$

Where  $p$  is the pressure (Pa),  $u$ , is the velocity component,  $u'$  is the velocity fluctuations, (m/s),  $x$  is the spatial coordinates (m),  $i, j$  are the spatial indices,  $\rho$  is the density ( $\text{kg/m}^3$ ),  $\mu$  is the dynamic viscosity ( $\text{kg/ms}$ ) and  $\mu_t$  is the turbulent viscosity ( $\text{kg/ms}$ ).

The k- $\omega$  SST turbulence model is a combined version of the k- $\epsilon$  and the k- $\omega$  turbulence models [18], and is governed by:

$$\frac{\partial}{\partial x_i} (\rho k u_i) = \frac{\partial}{\partial x_j} \left[ \left( \mu + \frac{\mu_t}{\sigma_k} \right) \frac{\partial k}{\partial x_j} \right] + G_k - Y_k + S_k \quad (4)$$

$$\frac{\partial}{\partial x_i} (\rho \omega u_i) = \frac{\partial}{\partial x_j} \left[ \left( \mu + \frac{\mu_t}{\sigma_\omega} \right) \frac{\partial \omega}{\partial x_j} \right] + G_\omega - Y_\omega + D_\omega + S_\omega \quad (5)$$

where  $k$  is turbulent kinetic energy ( $\text{m}^2/\text{s}^2$ ),  $\epsilon$  is the dissipated turbulent kinetic energy ( $\text{m}^2/\text{s}^3$ ),  $\omega$  is the specific turbulence dissipation rate ( $\text{m}^2/\text{s}$ ),  $\sigma_k$  is the generation of  $k$   $\sigma_\omega$  and is the generation of  $\omega$  due to mean velocity gradients,  $Y_k$  and  $Y_\omega$  represent the dissipation of  $k$  and  $\omega$  due to turbulence, respectively.  $S_k$  and  $S_\omega$  are user-defined source terms and  $D_\omega$  represents the cross-diffusion term.

The term  $G_k$  represents the production of turbulence kinetic energy due to mean velocity gradient that can be calculated by

$$G_k = -\rho \overline{u'_i u'_j} \frac{\partial u_j}{\partial x_i} \quad (6)$$

The production of  $\omega$  is given by equation

$$G_\omega = \beta \frac{\omega}{k} G_k \quad (7)$$

The coefficient  $\beta$  is a function of  $k$  and  $\omega$  and it is so calculated that in the far-field regions of flow approaches unity.

In order to compare the aerodynamic characteristics of different airfoil geometries, The lift and drag coefficients defined as [19]:

$$C_L = \frac{F_L}{\frac{1}{2} \rho u_\infty^2 c} \quad (8)$$

$$C_D = \frac{F_D}{\frac{1}{2} \rho u_\infty^2 c} \quad (9)$$

where  $c$  is the airfoil chord length (m),  $F_L$  is the lift force (N),  $F_D$  the drag force (N),  $u_\infty$  is the free stream velocity (m/s).

### 3. Computation Domain

The geometry of the smooth airfoil NACA0012 was prepared using coordinates taken from [20] and imported to DesignModeler of ANSYS. The C-shaped domain was considered around the airfoil with the given dimensions to obtain a domain-independent solution. Figure 1 shows a schematic diagram of the 2D computational domain with airfoil chord length ( $c$ ) of 1 meter.

The all surface modified shapes  $s$  were located at 75%  $c$  with a characteristic length of 3%  $c$ . Figure 2 shows a detailed dimensions for the semi-circle surface-modified airfoil used in the analysis.

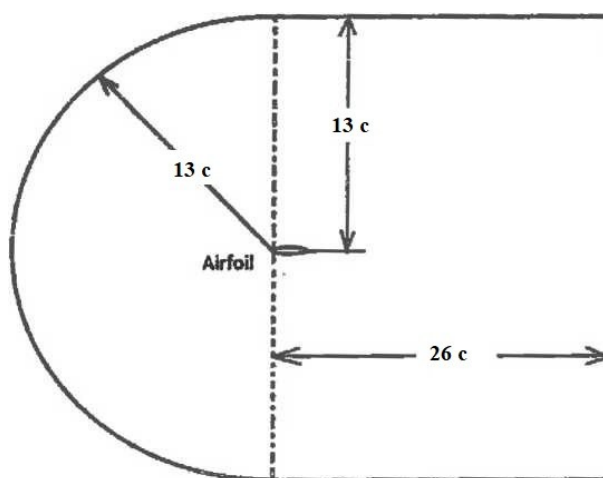


Figure 1: The C shaped computational domain

### 4. Solution Methodology

The CFD code ANSYS Fluent R1, was used to investigate the aerodynamic characteristics of the NACA0012 airfoil with surface modification. The airfoil was plotted by importing the data points and drawn by the DesignModeler component of the ANSYS software, and then the surface modification was designed on it. The chord length of the airfoil was one meter. The upper surface of the airfoil was modified by creating dimples and bumps with different shapes, placed at 75% of the chord. Domain meshing is done using hybrid unstructured mesh and the density of the mesh is greater near the wall region of the airfoil, as shown in Figure 3a. Inflation was used over the surface of airfoil, with first layer having a cell width of 0.01 mm. For precise simulation, the average value of  $y^+$  is kept under one ( $y^+ < 1$ ) for resolving the boundary layer on the mesh [21]. The SIMPLE algorithm was employed, with second-order upwind spatial discretization. The spatial gradient was selected as the least squares cell-based, and the  $k-\omega$  SST turbulence model was adopted. In the monitors section, convergence criteria are set such that the normalized residuals for each parameter are less than  $10E-6$  for higher accuracy. Standard initialization was used with declared inlet conditions to initialize the solution. The calculation was carried out for more than 2000 iterations, or until all scaled residuals were achieved. The boundary conditions of the computational domain were named according to the Figure 3b. The inlet conditions, where velocity inlet, no slip conditions are specified at the airfoil wall and pressure outlet at the outlet section.

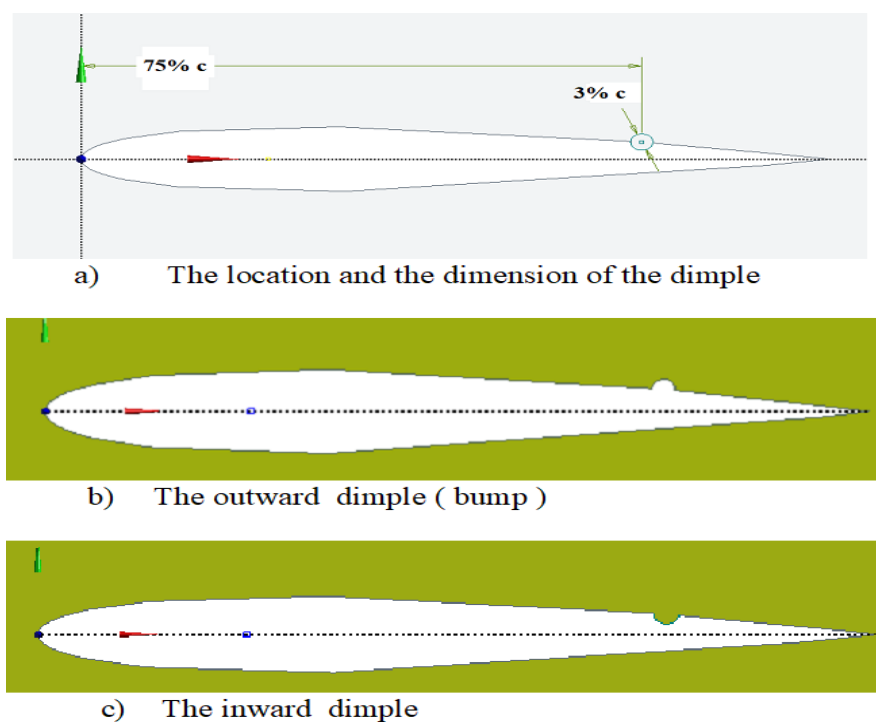


Figure 2: The details of the surface-modified airfoil with semi-circular dimple.

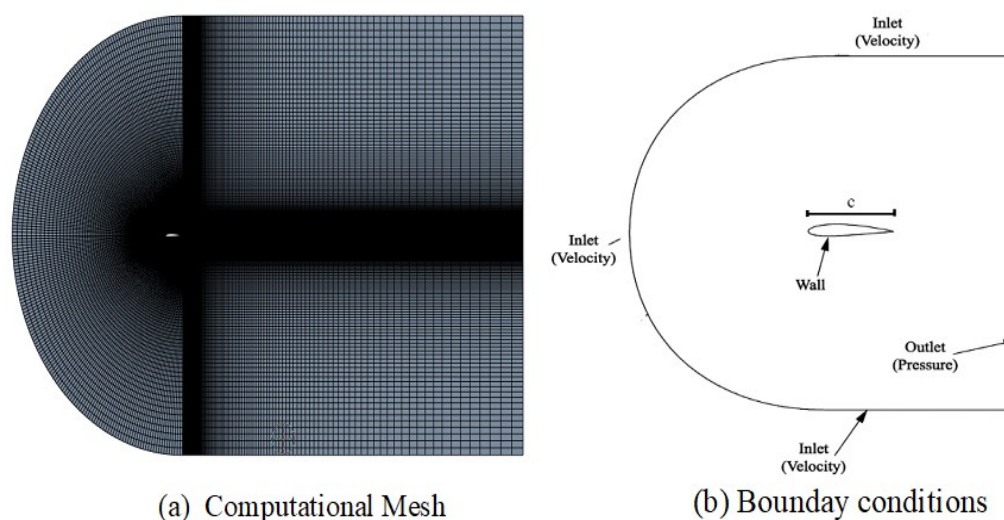


Figure 3: Computational domain meshing and boundaries.

## 5. Mesh Sensitivity and Code Validation

A grid independence study was conducted to select an optimum mesh number that guarantees the solution is independent of the mesh resolution. The mesh independence testing is performed and the mesh refinement is assessed using the lift coefficient variations. The test was carried out with  $3.0E + 6$  and  $\alpha = 15^\circ$ . Figure 4 shows the results of the test for each mesh. The fourth mesh is chosen for further computations.

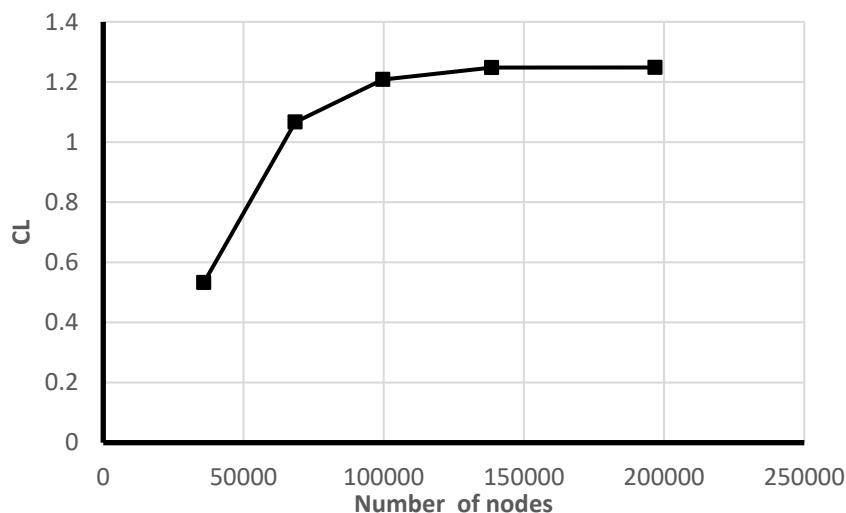


Figure 4: Grid independence testing

The pressure coefficient ( $C_p$ ) is plotted against  $x/c$  in Figure 5. The CFD results of the study compared with the experimental results of Ladson et al. [22] at zero angle of attack. It is found that the numerical results and experimental results are in good agreement, which indicates that the numerical simulation program is reliable.

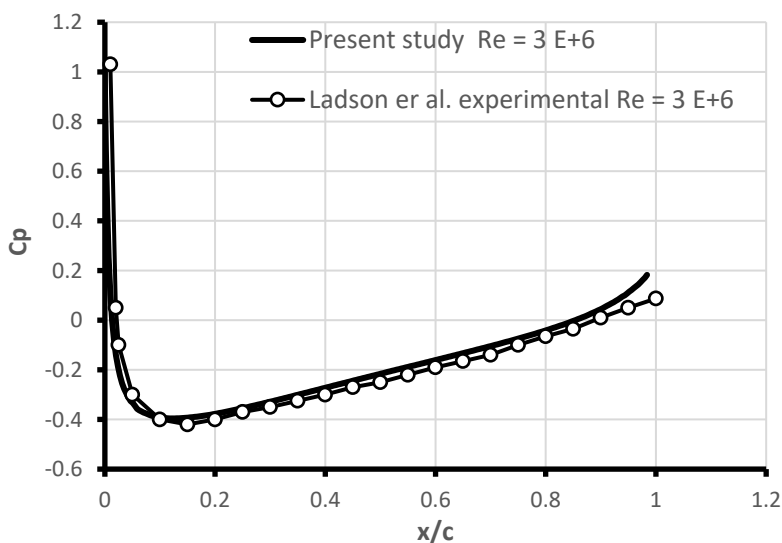


Figure 5: Pressure distribution model validation.

## 6. Results and Discussion

The results of the simulation of modified surfaces of the NACA 0012 airfoil with dimples and protrusions are presented in this section. Three different shapes were used namely, semicircular, v-shaped (triangular), square. The study was carried out with  $Re = 3.0E+6$ , located at  $0.75c$  and the range of attack angles was  $0 - 20^\circ$ .

### 6.1- Modified surface by dimples

The results of lift and drag coefficients of modified surface airfoils with respect to the smooth airfoil were investigated and analyzed. Lift and drag coefficients comparisons of surface dimples are shown in

Figures 6 and 7, respectively. All modified surfaces of airfoils, either by dimples or protrusions did not provide a better result at low angles of attack ( $0^\circ \leq \alpha \leq 10^\circ$ ). For higher angles of attack, in the near-stall region, there is an improvement in aerodynamic performance for all airfoils, where it can be seen an increase in lift coefficient and a reduction in drag coefficient. Since the flow along the surface of the airfoil enters a dimple, a small separation bubble is formed, causing acceleration of the flow between the dimples and boundary layer, resulting in a transition from laminar to turbulent. This transition leads to a delay in the separation of flow and improves the aerodynamic characteristics of the airfoil. All surface-modified airfoils have better performance than smooth airfoils. Comparing the shapes, the semi-circular dimple had a higher lift coefficient and a lower drag coefficient, indicating that it was a suitable modification for airfoil aerodynamic enhancement.

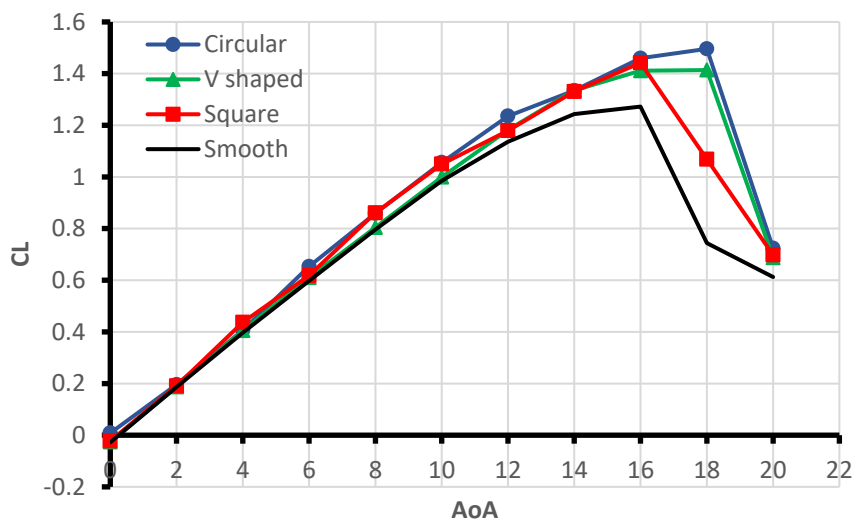


Figure 6: Lift coefficient for smooth and modified airfoils of different dimple shapes.

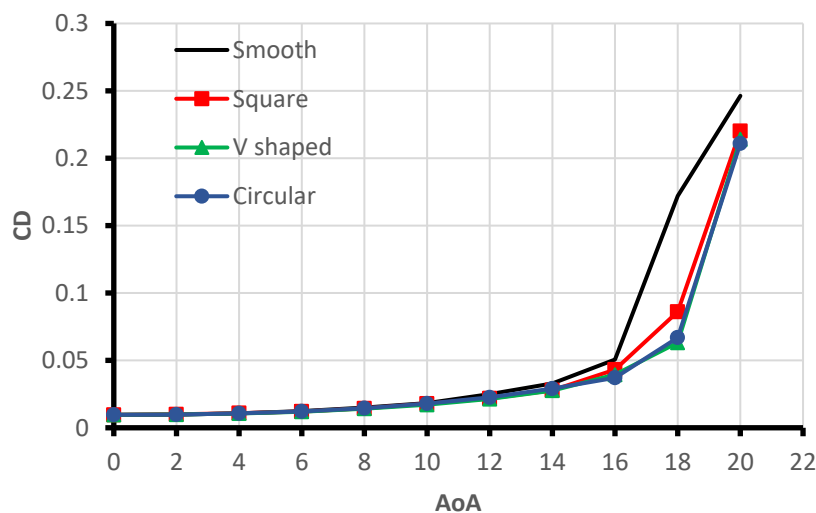


Figure 7: Drag coefficient for smooth and modified airfoils of different dimple shapes.

## 6.2 - Modified surface by protrusions

The characteristics of surface-modified airfoils with different shapes of vortex generators or protrusions (bumps) were compared. Comparisons between lift and drag coefficient of the modified and smooth

airfoils are shown in Figures 8 and 9, respectively. According to the analysis of the results, as seen in the dimpling case, there is no significant effect at low angles of attack. Then, at the near-stall region, the v-shaped vortex generator gives a lower drag coefficient and a higher lift coefficient near the stall region than the other shapes and also delays flow separation, which improves the stall angle by two degrees.

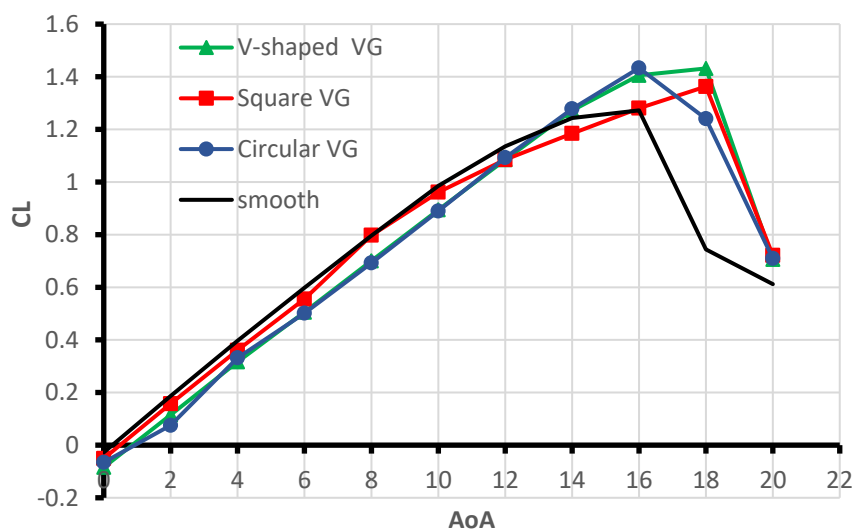


Figure 8: Lift coefficient for smooth and modified airfoils of different bump shapes.

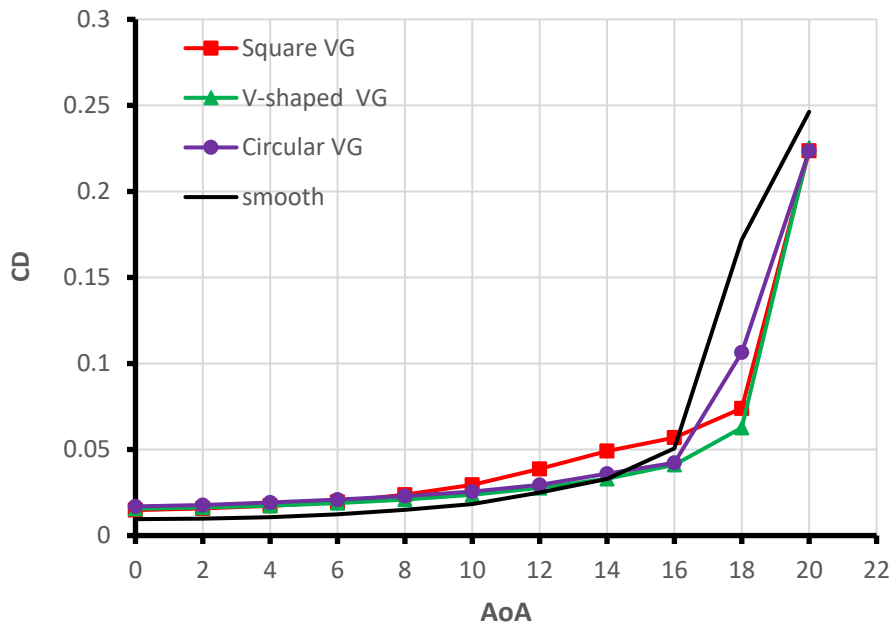


Figure 9: Drag coefficient for smooth and modified airfoils of different bump shapes.

### 6.3 - Modified surface comparison

Figures 10 and 11 show the static pressure and velocity magnitude contours of CFD simulations for smooth and surface-modified NACA 0012 airfoils, using various angles of attack. For all configurations,



at zero AoA, it can be observed that pressure and velocity distributions are similar on both sides of the airfoil. As a consequence, lift generation is also zero. As AoA increased, results showed that pressure on the upper side started decreasing while velocity increased, and on the lower side of the airfoil, the pressure started increasing while velocity decreased. As a result of the pressure difference between the airfoil sides, lift is generated, and the coefficient of lift increases with AoA. Also, separation of flow is gener.

Figures 10 and 11 show the static pressure and velocity magnitude contours of CFD simulations for smooth and surface-modified NACA 0012 airfoils, using various angles of attack. For all configurations, at zero AoA, it can be observed that pressure and velocity distributions are similar on both sides of the airfoil. As a consequence, lift generation is also zero. As AoA increased, results showed that pressure on the upper side started decreasing while velocity increased, and on the lower side of the airfoil, the pressure started increasing while velocity decreased. As a result of the pressure difference between the airfoil sides, lift is generated, and the coefficient of lift increases with AoA. Also, separation of flow is generated gradually at the trailing edge with AoA; as the AoA increases, the separation zone moves towards the leading edge, generating pressure drag. It is very evident that at higher AOA, the flow tends to separate from the trailing edge. The presence of dimples imparts turbulent kinetic energy, which helps in the reattachment of flow, and hence flow adheres to the airfoil surface. Modified surfaces by inward and outward dimples (bumps) act as vortex generators to create vortices so that the turbulent can be developed and delay the boundary layer separation of flow. Therefore, enhancing the aerodynamic characteristics of the airfoil. Aerodynamic performance was improved by reducing the pressure drag, increasing lift, and delaying the stall angle of attack. ated gradually at the trailing edge with AoA; as the AoA increases, the separation zone moves towards the leading edge, generating pressure drag. It is very evident that at higher AOA, the flow tends to separate from the trailing edge. The presence of dimples imparts turbulent kinetic energy, which helps in the reattachment of flow, and hence flow adheres to the airfoil surface. Modified surfaces by inward and outward dimples (bumps) act as vortex generators to create vortices so that the turbulent can be developed and delay the boundary layer separation of flow.

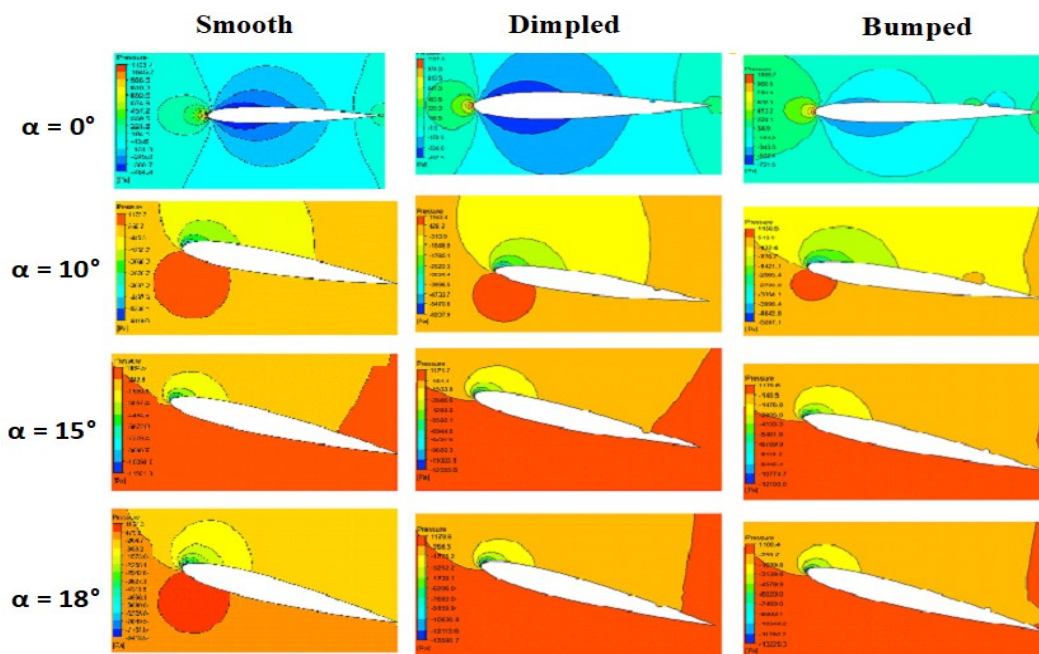


Figure 10: Pressure contours of smooth and modified surfaces of airfoil

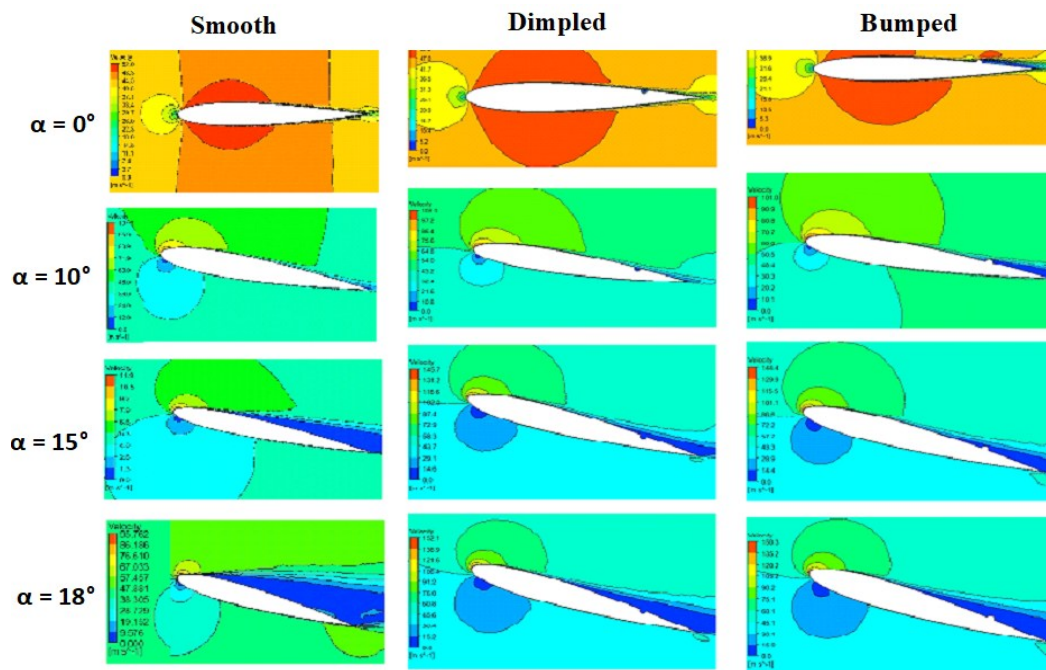


Figure 11: Velocity contours of smooth and modified surfaces of airfoil

Therefore, enhancing the aerodynamic characteristics of the airfoil. Aerodynamic performance was improved by reducing the pressure drag, increasing lift, and delaying the stall angle of attack.

A comparison was carried out between the two cases of surface modification, and the results are shown in Figures 12 and 13, for lift and drag coefficients, respectively. It is proven that having the dimple configuration has more benefits than vortex generators and adding a dimple to the airfoil does improve the aerodynamic characteristics of flow over symmetric airfoils.

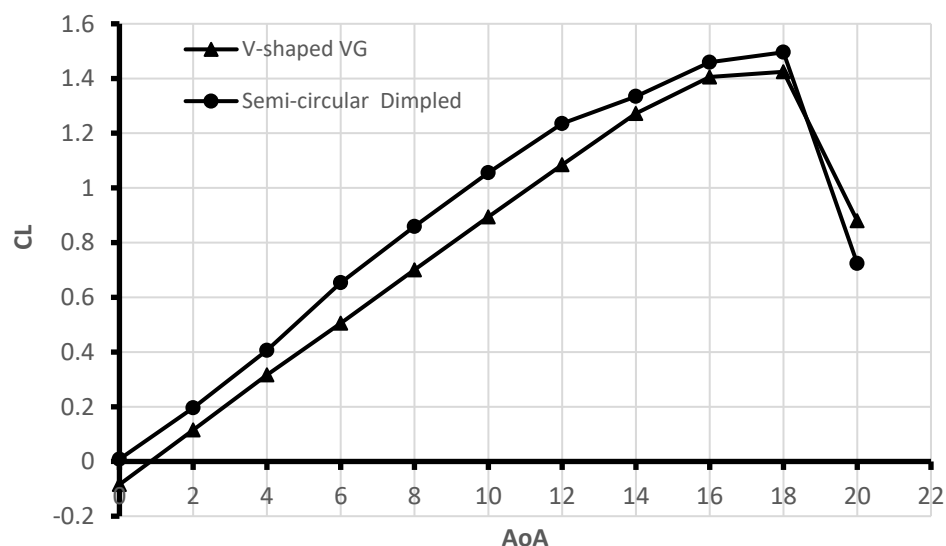


Figure 12: Lift coefficients comparison of dimpled and bumped airfoils.

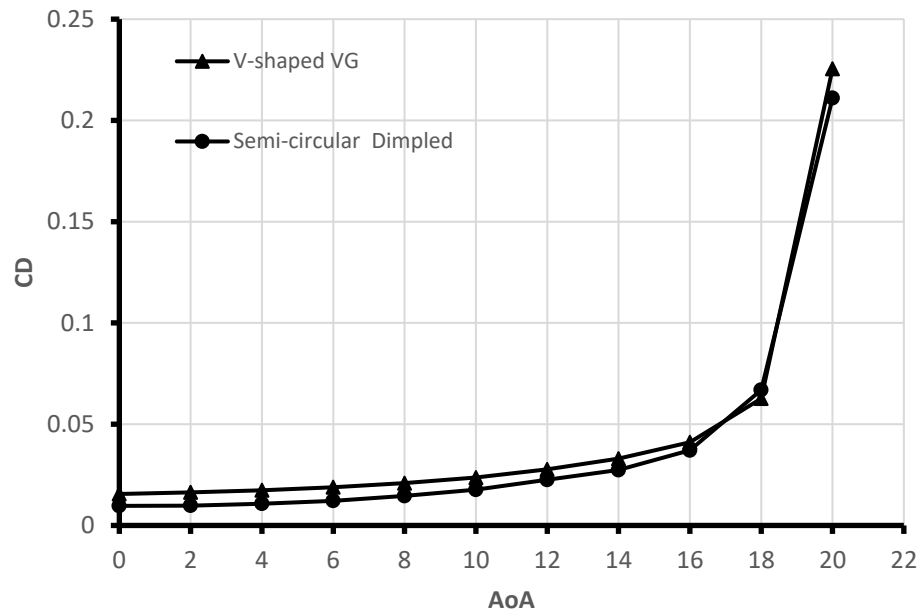


Figure 13: Drag coefficients comparison of dimpled and bumped airfoils.

## 7. Conclusions

ANSYS Fluent simulation study of the aerodynamic performance of surface-modified NACA0012 airfoils is presented and compared with a smooth airfoil. Three different shapes of dimples and protrusions were implemented at the 0.75  $c$  location and investigated at  $Re = 3E+6$  for various angles of attack. The modified surface airfoils showed an enhancement in aerodynamic performance compared to smooth airfoils, where the flow separation on the surface of the airfoil can be delayed by the surface modification. Semi-circular dimples with 3%  $c$  diameter located at 75%  $c$  on the upper surface of the airfoil showed an increase in the maximum lift coefficient of 11%, while the coefficient of drag was reduced by 3%. The airfoil with a dimple at 75% of chord length successfully controls the boundary layer separation, causing an increase in stall angle by 2 degrees. The v-shaped protrusion located at 75%  $c$  with a side length of 3%  $c$  has proven to have better aerodynamic enhancement than the other shapes. An increase of 9% in the total maximum lift coefficient and a decrease in drag coefficient up to 3% in the near-stall regime were reported for modification with a V-shaped bump at the upper surface of the airfoil. Also, there was an increase in the stall angle by 2 degrees. Among the surface modifications provided, the semi-circular dimple has better aerodynamic features than the v-shaped protrusion. Thus, dimples have proved to be more suitable than the protrusions. Effect of a changed Reynolds number can be investigated, especially at high velocity, so that the effect of compressibility is included. Also, other series of the airfoil can be simulated to investigate the effect of modifications.

## REFERENCES

- [1] Hare, H., Mebarki, G., Brioua, M., and M. Naoun, M., Aerodynamic performances improvement of NACA 4415 profile by passive flow control using vortex generators, *J. of Serbian Society for Comp. Mechanics*, 2019, vol. 13, No. 1, pp. 17 – 38.
- [2] Amit, K. S., Mahendra, P., and Chouhan, T., Review on Aerodynamic Behavior of Airfoil when Surface Modified, *Int. J. of Scientific & Engg. Res.*, 2016, pp. 516 – 519,
- [3] Wang, H., Zhang, B., Qiu, Q., Xu, X., Flow control on the NREL S809 wind turbine airfoil using vortex generators, *Energy*, 2017, vol. 118, pp. 1210 –1221.

- [4] Rajasai, B., Ravi T., and Srinath, S., Aerodynamic effects of dimple on aircraft wings”, *Int. J. Adv. Mech. Aero. Engg.*, 2015, vol. 2. no. 2, pp. 169 – 172.
- [5] Devi, B., and Shah, A. D., Computational Analysis of Cavity Effect over Aircraft wing, *World Engg. and App. Sci. J.*, 2017, vol. 8, no. 2, pp. 104 – 110.
- [6] Mustak, R., and Harun, M., Improvement of Aerodynamic Characteristics of an Airfoil by Surface Modification, *American J. of Engg. Res. (AJER)*, 2017, pp. 7 – 14.
- [7] Saraf, A.K., Singh, M.P., and Chouhanr, T.S., Study of Flow Separation on Airfoil with Bump, *Int. J. of App. Engg. Res.*, 2018, vol. 13, no. 16, pp. 868-872.
- [8] Cai, C., Zuo, Z., Liu, S., and Maeda, T., Effect of a single leading-edge protuberance on NACA 634021 airfoil performance, *J. of Fluids Engineering*. 2017, vol. 140, No. 2, pp. 021108 – 021115.
- [9] Kumar, G., Narayanan, K., Aravindhkumar. S., KishoreKumar, S., Comparative analysis of various vortex generators for a NACA 0012 airfoil, *Int. J. of Innovative Studies in Sci. and Engg Tech*. 2016, vol. 2, No. 5, pp. 3 – 6.
- [10] Fouatih, O., Medale, M., Imine, O., Imine, B., Design optimization of the aerodynamic passive flow control on NACA 4415 airfoil using vortex generators. *Eurp. J. of Mechanics-B/Fluids*. 2016, Vol. 56, pp. 82 – 96.
- [11] Mustak, R., Khan, M., Molla, M., Design and construction of NACA-4415 airfoil with various shaped surface modifications. *Asia Pacific J. of Engg. Sci. and Tech.*, 2017, vol. 3, no. 1, pp. 28 – 38.
- [12] Domel, G., Bertoldi, K., Saadat, M., Lauder, J.V., Weaver, J.C., and Haj-Hariri, H., Shark skin-inspired designs that improve aerodynamic performance, *J. R. Soc. Interface*, 2018, vol. 15, no. 139, pp. 1 – 9.
- [13] Rasal, S.K. and Katwate, R.R., Experimental Investigation of Lift and Drag Performance of NCAC 0012 Wind Turbine Aerofoil, *Int. Res. J. of Engg and Tech* , 2017, vol. 4, no. 6, pp. 265-270.
- [14] Vignesh, V., Vijaya M. G., Rishikesh. M., Analysis of Aerodynamic Characteristics on Surface Modification of Airfoil, *IJSART*, 2021, vol. 7 no. 8, pp. 47 – 50.
- [15] Omer, E.A.A., Momen, H. M., and Yahia, R.N, Aerodynamic Characteristics of Dimple Effect on Airfoil, *Academy J. for Basic and App. Sci. AJBAS*, 2023, vol. 5, no. 1, pp. 1 – 13.
- [16] Prasath. M. S., and Irish A. S., Effect of Dimples on Aircraft Wing, *Global Res. And Develop. J. for Engineering GRDJE*, 2017, vol. 2, No. 5, pp: 234-242.
- [17] Lars Davidson, Fluid mechanics, turbulent flow and turbulence modeling, Division of Fluid Dynamics, Department of Mechanics and Maritime Sciences, *Chalmers University of Technology*, SE-412 96 Goteborg, Sweden, 2022.
- [18] Hami, K., Turbulence Modeling a Review for Different Used Methods, *Int. J. of Heat and Tech.*, 2021, vol. 39, no. 1, pp. 227 – 234.
- [19] Anderson, J. D., FUNDAMENTALS OF AERODYNAMICS, McGraw Hill Series, 3<sup>rd</sup> ed, 2012.
- [20] <http://airfoiltools.com/airfoil/naca4digit>. (Accessed March, 2023).
- [21] ANSYS FLUENT THEORY GUIDE 2019, ANSYS, Inc.: Canonsburg, PA, USA.
- [22] Ladson, C. L., Hill, A. S., and Johnson, Jr., W. G., Pressure Distributions from High Reynolds Number Transonic Tests of an NACA 0012 Airfoil in the Langley 0.3-Meter Transonic Cryogenic Tunnel, NASA TM 100526, 1987